



**HAL**  
open science

## X-ray scattering by bicontinuous cubic phases

M. Clerc, E. Dubois-Violette

► **To cite this version:**

M. Clerc, E. Dubois-Violette. X-ray scattering by bicontinuous cubic phases. Journal de Physique II, 1994, 4 (2), pp.275-286. 10.1051/jp2:1994128 . jpa-00247961

**HAL Id: jpa-00247961**

**<https://hal.science/jpa-00247961>**

Submitted on 4 Feb 2008

**HAL** is a multi-disciplinary open access archive for the deposit and dissemination of scientific research documents, whether they are published or not. The documents may come from teaching and research institutions in France or abroad, or from public or private research centers.

L'archive ouverte pluridisciplinaire **HAL**, est destinée au dépôt et à la diffusion de documents scientifiques de niveau recherche, publiés ou non, émanant des établissements d'enseignement et de recherche français ou étrangers, des laboratoires publics ou privés.

Classification

Physics Abstracts

61.30 — 02.40 — 82.70

## X-ray scattering by bicontinuous cubic phases

M. Clerc and E. Dubois-Violette

Laboratoire de Physique des Solides (\*), Bâtiment 510, Université Paris-Sud, 91405 Orsay Cedex, France

(Received 18 June 1993, received in final form 13 October 1993, accepted 28 October 1993)

**Abstract.** — Ia3d bicontinuous cubic phases are interpreted as constituted of a fluid film of constant thickness supported by the gyroid minimal surface. We first compute the gyroid structure factor. Then we decorate the surface by the film. We compute the diffracted intensities and compare to X-ray intensities measured in some lipid systems.

### 1. Introduction.

Recently it has been shown that a large variety of cubic phases appearing in various biological or chemical systems can be described as triply-periodic bicontinuous phases. A panorama of all these systems is given in [1]. Such cubic phases appear for example in lyotropic compounds between the lamellar and the hexagonal phases [2-4]. They are different from the micellar cubic phases which exist in another part of the phase diagram and which are not bicontinuous. Following a similar scenario bicontinuous cubic phases with an analogous morphology appear in copolymer systems [1, p. 363] and phasmidic compounds [1, p. 229].

The common feature to all these phases is the importance of interfaces and the fact that mostly three space groups are observed : Ia3d, Pn3m and rarely the space group Im3m. It has been shown that these systems can be described in terms of a crystallography of films [1, p. 83, 5, 6] (or surfaces) and that good candidates for that were some infinite periodic minimal surfaces (I.P.M.S.) [7-9]. It also appeared that the structure of the two cubic blue phases of thermotropic liquid crystals could be described with use of the above I.P.M.S. [10]. The three cubic I.P.M.S. with the above space groups are the well-known gyroid G [11], F and P [12] I.P.M.S. They divide the space into two infinite, unconnected but mutually interwoven periodic labyrinths. Most of the experiments allowing the determination of the space groups are X-ray diffraction experiments or electron microscope image analysis. Then, to compare models linked to I.P.M.S. with experiments, we need to know the structure factor of these interfaces. The structure factors of the P and F surfaces are known [13] but not that of the G surface, which corresponds to the space group Ia3d commonly encountered in biologic

---

(\*) Associé au CNRS.

systems [1, p. 35]. For lipid samples Luzzati and Spert [14] proposed a structure with rods defining two infinite 3D-networks unconnected but mutually interwoven. These rods are somehow the cores of the minimal surface G. Both descriptions in terms of rods or I.P.M.S. appear to be complementary. The main conceptual difference between these two models is that interfaces built around I.P.M.S. are smooth curved surfaces, as is expected for fluid interfaces, contrary to cylindrical rods joining at vertices [15] which give curvature only on singularity lines. This point may be of importance if one considers the interfaces of the cubic phases as resulting from the release of a geometrical frustration in a curved space [5, 6].

The aim of this paper is to consider the G surface as the skeleton around which interfaces of Ia3d cubic structures organize themselves. Section 2 is devoted to the determination of the structure factor of the interface skeleton (G surface). In section 3 we give a simple model in order to compute the intensity scattered by a film of constant thickness supported by the minimal surface. We introduce a decoration of the surface with spheres and link the geometrical parameters of the model to those of the minimal surface. In section 4 we focus our attention to lyotropic systems. We examine the case of direct and inverse phases and compare the calculated diffracted intensities to those measured in X-ray experiments [15].

## 2. Structure factor of the gyroid surface.

Minimal surfaces can be generated by a set of equations giving their Cartesian coordinates  $\mathbf{r} = (x, y, z)$  in terms of a complex variable  $\omega$  as first given by Weierstrass

$$\mathbf{r}(\omega) = \mathbf{r}_0 + \text{Re} \left[ \mu \int_{\omega_0}^{\omega} f(\omega) \mathbf{R}(\omega) d\omega \right], \quad (1)$$

where  $\mu = \gamma \exp[i\alpha]$ ,  $x, y, z$  are dimensionless coordinates ( $\mathbf{r} = \mathbf{R}/a$ ,  $\mathbf{R}$  defines the position of a point on the surface and  $a$  is the cubic cell parameter) and  $f_x(\omega) = 1 - \omega^2$ ,  $f_y(\omega) = i(1 + \omega^2)$ ,  $f_z(\omega) = -2\omega$ .

Each minimal surface is defined by the complex function  $R(\omega) \exp(i\alpha)$ . The function  $R(\omega) = (1 + 14\omega^4 + \omega^8)^{-1/2}$  is the same [1, p. 237] [10] for the three surfaces P, G and F, which transform in one another by changing the value of  $\alpha$  (Bonnet transformation) [16]. The P, G and F surfaces are obtained for  $\alpha = 0$ ,  $\alpha = 51.985^\circ$ ,  $\alpha = 90^\circ$ . It has been proved that these surfaces could be generated with a unique surface in  $\mathbf{C}^3 \sim \mathbf{R}^6$  [17]. The three I.P.M.S. then correspond to a projection in  $\mathbf{R}^3$ , defined by the angle  $\alpha$ .

For the G surface, the dimensionless number  $\gamma^{-1}$  equals 2.65624.

STRUCTURE FACTOR. — The dimensionless structure factor  $F_{hkl}^{\text{MS}}$  of the minimal surface reads

$$F_{hkl}^{\text{MS}} = \int_{S_0} \exp^{2\pi i \mathbf{s} \cdot \mathbf{r}} d\sigma, \quad (2)$$

where  $d\sigma$  is the surface element,  $\mathbf{S}$  is the scattering vector, or in reduced units  $d\sigma = d\Sigma/a^2$ ,  $\mathbf{s} = \mathbf{S}/a$  with  $s^2 = h^2 + k^2 + \ell^2$ . Since the minimal surface is periodic the integral of equation (2) has to be performed on the surface  $S_0$  of the minimal surface contained in the cubic unit cell. It may be expressed in terms of the two real coordinates  $u = \text{Real}(\omega)$ ,  $v = \text{Im}(\omega)$  in the Weierstrass plane.  $\mathbf{r}$  is computed with use of equation (1) and the surface element  $d\sigma = t^2(\omega) du dv$  is expressed with the Jacobian [10]  $t(\omega) = \gamma |R(\omega)| (1 + \omega \bar{\omega})$ .

Taking into account the symmetry operations of the space group we only perform the integration in the sector (Fig. 1) of the Weierstrass plane which generates the part of the surface

contained in the asymmetric unit. By definition the asymmetric unit allows us to rebuild the whole cubic cell by application of the 96 symmetry operations of the Ia3d group.

Let us point out that the symmetry operations defined in the crystallographic tables imply a well defined origin (point O in Fig. 1). We checked the program by performing a similar integration for the P surface for which results are known [13]. The precision of the calculus is estimated from the comparison between  $F_{000}$  and the theoretical value of the reduced surface  $\sigma_c = A_c / \Omega_c^{2/3} = 3.091$  [12] where  $\Omega_c = a^3$  and  $A_c$  is the surface contained in the cubic cell. Notice that  $\sigma_c = 2^{1/3} \sigma_p$  where  $\sigma_p = 2.453$  is the value for the primitive cell. We performed the integration with a mesh of the surface leading to a precision of  $10^{-3}$  on the amplitudes. We give the results for the first 17 amplitudes in table I.

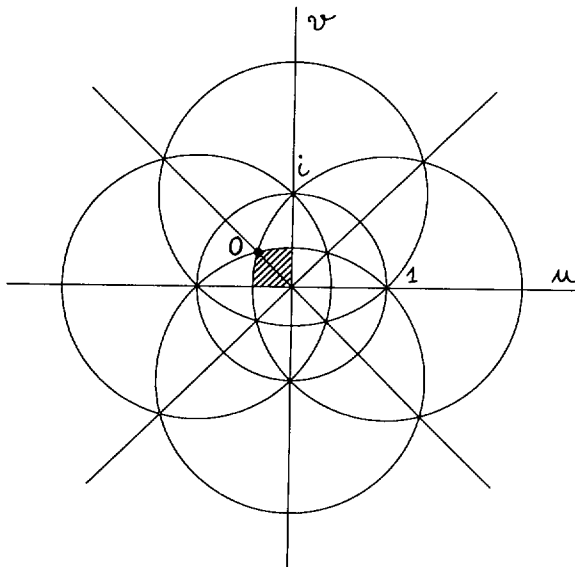


Fig. 1.

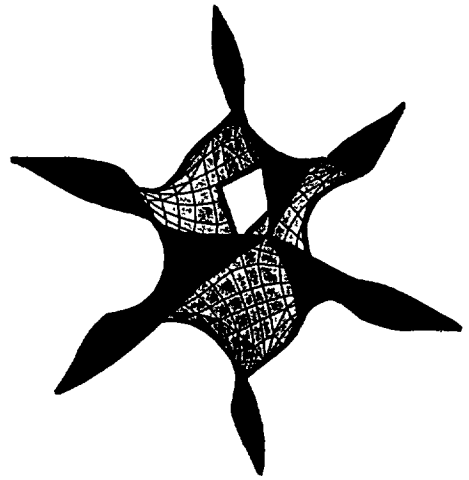


Fig. 2.

Fig. 1. — Weierstrass plane. The dashed region is the domain of integration corresponding to the asymmetric unit represented in figure 2.

Fig. 2. — Primitive cell with the asymmetric unit in white (with some hidden part). The origin of the cell corresponds to the (hidden) lower vertex of the asymmetric unit.

### 3 X-ray intensities diffracted by a film of constant thickness.

3.1 DECORATION OF THE MINIMAL SURFACE. — We decorate the skeleton of the minimal surface with a film of constant thickness and restrict the description to a model with two densities ( $\rho_1$  and  $\rho_0$  are the densities inside and outside of the film). An exact way to introduce the decoration of the minimal surface with a film of constant thickness  $2\ell$  and constant density takes into account the normal vector  $N$  at any point  $R_0$  of the minimal surface. The dimensionless diffracted amplitude  $F_{h\lambda\ell}$  then is

$$F_{h\lambda\ell} \approx \frac{1}{2\ell} \int_{-\ell}^{+\ell} \int_{S_0} e^{2\pi i S(R_0 + \lambda N)} d\sigma d\lambda . \tag{3}$$

Table I. — *The computed G structure factor for the first 17 reflections. M is the multiplicity of the (hkl) reflection family.  $M |F_{hkl}^{MS}|^2$  would correspond to a powder diagram intensity.*

## G Surface

hkl	$F_{hkl}^{MS}$	M(hkl)	$M  F_{hkl}^{MS} ^2$
211	+0.660	24	10.454
220	+0.451	12	2.441
321	-0.092	48	0.406
400	-0.360	6	0.778
420	-0.338	24	2.742
332	+0.467	24	5.234
422	+0.282	24	1.909
431	+0.209	48	2.097
521	-0.077	48	0.285
440	-0.060	12	0.043
611	-0.245	24	1.441
532	-0.104	48	0.519
620	-0.060	24	0.086
541	-0.162	48	1.26
631	-0.199	48	1.901
444	+0.395	8	1.248
543	+0.302	48	4.378

This description leads to tedious calculations since it does not lead, in the diffraction factor, to the factorization of the contributions coming from the skeleton (I.P.M.S.) and from the decoration (the film). In order to get a mathematical simplification (factorization) we perform the decoration in a simple manner which avoids a description including the normal vector at any point of the I.P.M.S. We introduce an isotropic decoration around each point  $\mathbf{R}_0$  of the minimal surface with spheres of radius  $R_s$  and with a spherical distribution of the density  $\rho_s(|\mathbf{R}|)$  at a point  $\mathbf{R}$  of the sphere. This process describes a film of constant thickness  $2R_s$ . The density profile in the film depends (as we shall see later) on the overlap of the spheres and on the precise form of the density distribution  $\rho_s(|\mathbf{R}|)$  for one sphere.

The density at a point  $\mathbf{M}$  of the film is

$$\rho(\mathbf{OM}) = \int \int \rho_s(|\mathbf{R}|) \delta(\mathbf{OM} - (\mathbf{R}_0 + \mathbf{R})) d^3\mathbf{R} d^3\mathbf{R}_0 \quad (4)$$

where  $\mathbf{R}$  is a point of the sphere. The dimensionless diffracted amplitude then is factorized as

$$F_{hkl} \approx \frac{1}{a^2} \int_{\text{Sphere}} \rho_s(|\mathbf{R}|) e^{2\pi i \mathbf{SR}} d^3\mathbf{R} \int_{S_0} e^{2\pi i \mathbf{SR}_0} d\Sigma$$

or with use of equation (2)

$$F_{hkl} \approx F_{hkl}^{\text{Sphere}} F_{hkl}^{\text{MS}} . \tag{5}$$

$F_{hkl}^{\text{Sphere}}$  is the Fourier transform of a sphere with a density distribution  $\rho_s(\mathbf{R})$ . We have chosen a model with spheres with a constant surfacial density  $\beta_s$ . This simply leads to

$$F_{hkl}^{\text{Sphere}} = 4 \pi \beta_s R_s^2 \frac{\sin(2 \pi s r_s)}{(2 \pi s r_s)} , \quad r_s = \frac{R_s}{a} \tag{6}$$

which is the Fourier transform of a rectangular function of width  $2 r_s$ .

Let us now justify the choice of a constant surfacial density for the spheres. We show that, neglecting second-order terms in curvature, this distribution induces a constant density profile in the film of thickness  $2 r_s$ . At each point of the surface, we neglect the Gaussian curvature i.e. we approximate locally the surface to a plane portion. Then all the spheres give the same contribution to the density in a small layer of thickness  $dz$  at position  $z$  along the normal to the plane (Fig. 3). If  $n_s$  is the number of centers of spheres per unit area one obtains the density  $dm$  in the thickness  $dz$  as

$$dm = n_s \beta_s 2 \pi R_s \sin \theta R_s d\theta \quad \text{or} \quad dm = -2 \pi n_s \beta_s R_s dz .$$

This leads to a constant density profile in the film (in Fig. 4) [19]

$$\rho(z) = n_s \beta_s 2 \pi R_s = \rho_1 \quad \text{for} \quad |z| < R_s . \tag{7}$$

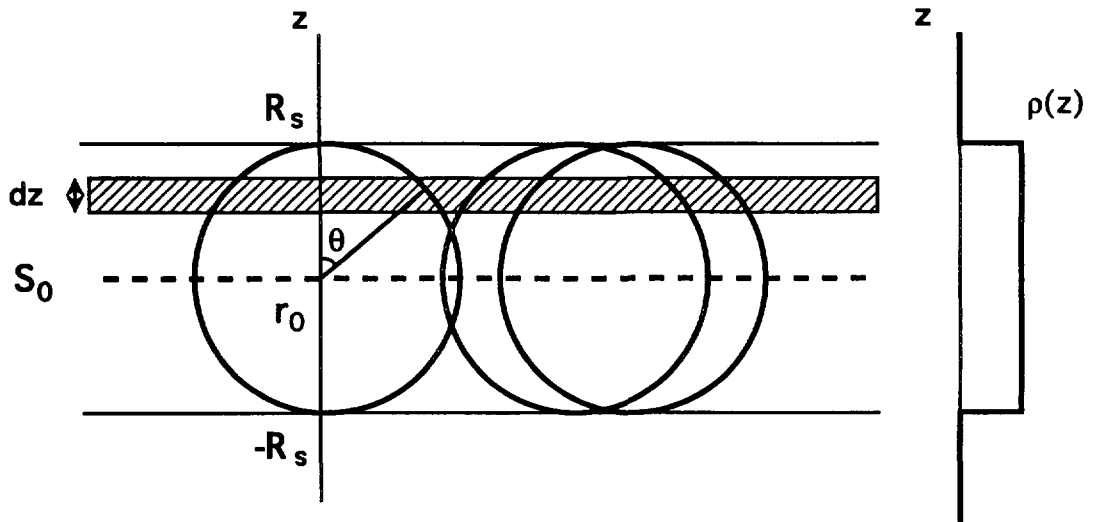


Fig. 3. — Density profile  $\rho(z)$  induced by spheres with constant surfacial density  $\beta_s$ . All spheres give the same contribution in a small layer of thickness  $dz$ .

**3.2 STRUCTURE FACTOR OF THE FILM.** — We also introduce a Debye-Waller factor in order to take into account some thermic disorder characterized by the dimensionless displacement  $u = \Delta U/a$  of the film. The total intensity for a powder diagram reads

$$I_{hkl}^{\text{tot}} = \lambda M(hkl) |F_{hkl}^{\text{MS}}|^2 |F_{hkl}^{\text{Sphere}}|^2 \exp^{-\alpha s^2} , \tag{8}$$

where  $\alpha = \frac{2 \pi^2}{3} \langle \mathbf{u}^2 \rangle$ ,  $M(hk\ell)$  is the multiplicity of the reflection  $hk\ell$  and  $\lambda$  is a scaling factor.

**3.3 GEOMETRICAL PARAMETERS OF THE FILM.** — Let us now describe the geometrical parameters of a film of constant thickness  $2\ell$  supported by the minimal surface as seen in figure 4. We can express the volume  $V_p$  of the film and the surface  $\Sigma_p = \Sigma_+ + \Sigma_-$  of the two interfaces in the primitive cell in terms of  $\ell$  and of quantities linked to the minimal surface. Let us consider a surface element  $d^2A_0$  at a point where the curvature radius is  $R_0$ , we get easily for the minimal surface ( $d^2\Sigma_- = d^2\Sigma_+$ )

$$d^2\Sigma = d^2\Sigma_- + d^2\Sigma_+ = 2 d^2\Sigma_- = 2 \left( 1 - \frac{\ell^2}{R_0^2} \right) d^2A_0 \tag{9}$$

$$d^3V = \int_0^\ell d^2\Sigma du = 2 \left( \ell - \frac{\ell^3}{3 R_0^2} \right) d^2A_0 \tag{10}$$

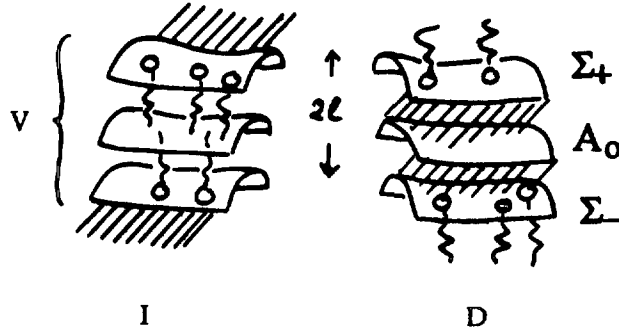


Fig. 4. — Film of direct (D) and inverse (I) phases.  $A_0$  is the minimal surface.  $\Sigma_+$  and  $\Sigma_-$  are surfaces parallel to  $A_0$  at a distance  $\ell$ .  $V$  is the volume enclosed by the film. The dashed regions correspond to the water.

$V_p$  and  $\Sigma_p$  are obtained by integration of equations (9) and (10) over the primitive cell, with the use of the Gauss-Bonnet theorem :

$$\int_{\text{Primitive cell}} - \frac{d^2A_0}{R_0^2} = 4 \pi (1 - g) \tag{11}$$

where  $g$  is the genus of the minimal surface equal to 3 for the three surfaces P, G, F. This leads for reduced parameters for the cubic cell (twice the primitive cell)  $s_c = \frac{\Sigma_c}{a^2} = \frac{2 \Sigma_p}{a^2}$ ,

$$v_c = \frac{V_c}{a^3} = \frac{2 V_p}{a^3}.$$

$$s_c = 2(\sigma_c - 16 \pi p^2) \tag{12}$$

$$v_c = 2 \left( \sigma_c p - \frac{16 \pi p^3}{3} \right). \tag{13}$$

Let us emphasize that the geometrical parameters of the film around the minimal surface only depend on one parameter, its reduced thickness  $2p = 2\ell/a$ . The model will be valid if the

radius of the sphere  $R_s$  is smaller than the curvature radius  $R_0$  i.e.  $p < r_0$ . Minoration of  $r_0 = \frac{\gamma}{2a} |R(\omega)| (1 + \omega \bar{\omega})^2$  in the Weierstrass plane gives  $r_0 > 0.188$ . Another estimate is obtained from the mean curvature radius calculated with the use of the Gauss-Bonnet theorem (Eq. (11))

$$\int_{\text{Primitive cell}} -\frac{d^2 A_0}{R_0^2} = 4 \pi (1 - g) = \left\langle \frac{1}{R_0^2} \right\rangle \int d^2 A_0.$$

We obtain  $\frac{\sqrt{\langle R_0^2 \rangle}}{a} = 0.25$ . We shall then impose in the following fits  $p < 0.25$ .

#### 4. X-ray intensities diffracted by Ia3d lipid cubic phases.

For lipids systems the film which decorates the minimal surface is a film of water (containing the polar heads) for direct phases and a film of paraffinic chains for inverse phases. The calculated intensities (Eq. (8)) depend on two parameters : the film thickness  $2 r_s$  and the strength of the thermal disorder  $\alpha$ . We shall now focus our discussion on the parameter  $p$  which can be deduced either from macroscopic measurements or from an estimate of the molecular parameters. For macroscopic criteria we use the relation

$$\Omega_c = V_w + V_{\text{part}},$$

where  $V_w$  and  $V_{\text{part}}$  are the volume respectively occupied by the water and by the paraffinic chains. The macroscopic measurement commonly given in the literature [15, 20] is the volume fraction  $C_{v, \text{pol}} = V_w / \Omega_c$  occupied by the water. The molecular parameters are the volume  $v_0$  occupied by one paraffinic chain and the surface  $s_0$  occupied by one polar head.

4.1 DIRECT PHASE. —  $V_c = V_w$  and equation (13) is simply

$$C_{v, \text{pol}} = v_c = 2 \left( \sigma_c p - \frac{16 \pi p^3}{3} \right). \quad (14)$$

To relate  $p$  to the molecular parameters we use  $V_{\text{part}} = N v_0$  where  $N = \Sigma_c / s_0$  is the number of paraffinic molecules contained in the cubic cell. Simple algebra leads to the dimensionless equation for  $p$

$$-\frac{16 \pi}{3} p^3 - 16 \pi m p^2 + \sigma_c p + m \sigma_c - \frac{1}{2} = 0, \quad \text{with } m = v_0 / s_0 a. \quad (15)$$

4.2 INVERSE PHASE. —  $V_{\text{part}} = V_c$  which leads, with use of equation (13) to

$$1 - C_{v, \text{pol}} = 2 \left( \sigma_c p - \frac{16 \pi p^3}{3} \right). \quad (16)$$

Estimation of  $p$  in terms of the molecular parameter is straightforward as  $\frac{v_c}{s_c} = m$ . Combining equations (12) and (13) we obtain

$$\frac{16 \pi}{3} p^3 - 16 \pi m p^2 - \sigma_c p + m \sigma_c = 0. \quad (17)$$



**4.3 COMPARISON WITH EXPERIMENTS.** — We now want to compare the above I.P.M.S. model with the experimental data of Ia3d structures, namely the two direct and three inverse lipid phases of references [14, 15]. Observations and results are summarized in tables II, III and IV. Let us first note that the I.P.M.S. model gives a prediction for the amplitude signs. This has to be compared with the signs deduced in very nice recent experiments [20] by confrontation of the electron density profile computed from X-ray diffraction analysis with freeze-feature electron micrographs. The  $F_{hkl}^{MS}$  signs and those selected in [20] are in complete agreement for the first 10 reflections. This is not the case for the complementary model with rods [14]. At first sight it seems to be in favour of the I.P.M.S. model. But one has to be aware of the decoration influence. A modification of  $r_s$  changes the signs *via* the oscillations of  $\sin(2\pi r_s s)/(2\pi r_s s)$  (Eq. (6)). In our cases this occurs for  $sr_s = 0.5$  this and affects the signs after the 10<sup>th</sup> peak, as can be seen in details in tables II, III and IV.

As we claimed earlier, the theoretical intensities depend on two parameter  $r_s$ ,  $\alpha$  and on an arbitrary scaling factor  $\lambda$ . Let us emphasize that  $2r_s$  in the model with the above decoration is the film thickness. We have determined these factors in order to fit at best the data, using a least mean square fit criterion. In each case we have computed the factor

$$\Delta = \left[ \sum_i \frac{(I_{i,cal} - I_{i,obs})^2}{N} \right]^{1/2}$$

where  $I_{i,cal}$  and  $I_{i,obs}$  are the theoretical and observed intensities of the  $i$ -th reflection.  $N$  is the total number of reflections.

For each compound we have verified (Tab. V) the agreement between the  $r_s$  value determined by the fit on intensities and the  $p$  value derived from macroscopic [15, 20] or microscopic data [21] using equations (14) to (17). The calculated intensities for the decorated I.P.M.S. fit quite well the data and the  $\Delta$  values do not greatly exceed the uncertainty on the measured intensities.  $\Delta$  values obtained for the rod model are much larger than that deduced from the I.P.M.S. model. However the rod model does not take the (211) reflection properly into account. On the contrary the I.P.M.S. model takes all the reflections into account and focus on the most intense ones. Nevertheless in order to perform the comparison between the two models we have also performed a fit excluding the (211) reflection and leading to different sets of intensities  $I_{ms}^*$  and  $\Delta^*$  values. In order to lighten the presentation we only give in detail the resulting intensities for the Gal compound. The  $\Delta^*$  values for the two models then become more comparable but nevertheless still with better values for the I.P.M.S. model. Let us note that results for the I.P.M.S. model are all the more satisfying since it only includes two parameters, contrary to three in the rod model. The radius of the cylinders  $r$  around the rod plays a role similar to that of the radius of the sphere  $r_s$  in the I.P.M.S. model.  $\alpha$  is the same parameter in the two models. The extra parameter  $\varepsilon$  in the rod model is the gap of the cylinder length introduced at each end of the rods [15].

## 5. Conclusion.

In this paper we give an interpretation of the X-ray diffraction patterns observed in cubic phases with symmetry group Ia3d within the frame work of models linked to minimal surfaces. The governing idea is the organization of films around the gyroid minimal surface taking into account the curvature of the interfaces. In this spirit we have computed the structure factor of the  $G$  minimal surface. The result for the series of amplitude signs is note worthy. Indeed this series corresponds to a relevant density map selected in [20]. The simple sphere model is promising since the associated intensities fit the experimental data quite well. It would be of

Table II. — Inverse phases.  $I_{\text{obs}}$ , observed intensities reported from [15].  $I_{\text{rod}}$ , fit by the rod model from [15].  $I_{\text{ms}}$ , fit by the I.P.M.S. model.  $\Delta = \left[ \sum_i \frac{(I_{i, \text{cal}} - I_{i, \text{obs}})^2}{N} \right]^{1/2}$  where  $N$  is the total number of reflections.  $\Delta^*$  corresponds to a fit for the I.P.M.S. model excluding the (211) reflection.  $r$ : (dimensionless quantity) is the sphere radius  $r_s$  in the I.P.M.S. model and a cylinder radius in the rod model.  $\alpha$ : Coefficient in the exponential Debye-Waller term.  $D$  column: Amplitude sign derived from [20].  $MS$  column: Amplitude sign for the I.P.M.S. model.  $\Sigma_i I$  is the sum of the intensities.

SrC<sub>14</sub>

hkl	$I_{\text{obs}}$	$I_{\text{rod}}$	$I_{\text{ms}}$	D	MS
211	12350	10000	12355	-	+
220	1020	975	922	-	+
321	48	43	17	+	+
400	145	333	88	+	+
420	794	1950	595	+	+
332	1205	2040	1216	-	-
422	333	470	432	-	-
431	208	110	431	-	-
521	<10	5	41	0	+
440	<10	5	5	0	+
611	{ 259	{ 376	50	-	+
532			18	-	+
620	<10	1	2	0	+
541	132	152	12	-	+
631	118	173	1	-	+
444	60	91	0	+	+
543	187	155	5	+	+
$r$		0	0.145		
$\Delta$		672	110		
$\Delta^*$		363	75		
$\Sigma_i I$	16859	16879	16190		
$\alpha$		0.044	0.037		

Table III. — *Inverse phases. Notation is the same as in table II.*

Lecithin						Galactolipids						
hkl	I <sub>obs</sub>	I <sub>rod</sub>	I <sub>m s</sub>	D	MS	hkl	I <sub>obs</sub>	I <sub>rod</sub>	I <sub>m s</sub>	I <sub>ms</sub> *	D	MS
211	12000	10000	12022	-	-	211	1800	10000	1830	3060	-	-
220	2080	520	1933	+	-	220	520	520	342	519	-	-
321	104	115	87	+	+	321	35	21	27	30	+	+
400	52	67	98	+	+	400	31	17	39	38	+	+
420	<20	26	89	0	+	420	40	24	72	52	+	+
332	<20	3	64	0	-	332	56	70	95	57	-	-
422	<20	2	5	0	-	422	7	22	23	11	-	-
431	<20	3	0	0	-	431	<7	9	15	5	0	-
521	<20	3	2	0	-	521	<7	2	0	0	0	+
440	<20	10	0	0	-	440	<10	9	0	0	0	+
611	{ 133	143	37	-	-	611	{ 24	127	1	3	+	-
532		1	13	-	-	532		0	1	-	-	
620	<25	38	3	0	-	620	<12	0	0	0	0	-
541	48	21	40	+	-	541	20	34	3	4	+	-
631	78	49	64	-	-	631	20	28	10	9	-	-
444		42	42	-	+	444		21	8	6	+	+
543	81		142	+	+	543	30	22	35	22	+	+
r		0.129	0.098			r		0.14	0.085	0.09		
Δ		614	53			Δ		1987	46			
Δ*		390	26			Δ*		22		8		
Σ <sub>i</sub> I	14576	11043	14641			Σ <sub>i</sub> I	2604	10926	2500	3817		
α		0.036	0.03			α		0.038	0	0.032		

interest to describe more precisely a film of constant density around the minimal surface. This would lead to a more sophisticated model taking into account the local properties (normal and curvature) of the surface (Eq. 3) [22]. Details of the density profile (polar heads contribution...) could also be introduced. These refinements would be of interest only in comparison with precise intensity measurements on Ia3d structures for different compounds.

Table IV. — Direct phases. Notation is the same as in table II.

KC <sub>12</sub>						C <sub>16</sub> TAB					
hkl	I <sub>obs</sub>	I <sub>rod</sub>	I <sub>m s</sub>	D	MS	hkl	I <sub>obs</sub>	I <sub>rod</sub>	I <sub>m s</sub>	D	MS
211	7320	10000	7317	+	+	211	6000	10000	6035	+	+
220	980	980	1002	+	+	220	1280	1280	1051	+	+
321	12	6	30	-	-	321	14	13	65	-	-
400	16	7	31	-	-	400	10	6	85	-	-
420	31	27	28	-	-	420	30	31	124	-	-
332	85	117	24	+	+	332	59	120	138	+	+
422	25	70	4	+	+	422	11	51	26	+	+
431	14	30	1	+	+						
r		0.16 0.18	0.09			r		0.17 0.2	0.09		
Δ		948	25			Δ		1513	105		
Δ*		22	20			Δ*		30	19		
Σ <sub>i</sub> I	8483	11237	8437			Σ <sub>i</sub> I	7404	11501	7524		
α		0.047	0.14			α		0.104	0.019		

Table V. — Estimate of the parameter  $p$ . —  $p_1$  is derived from equation (14) (respectively Eq. (16)).  $C_{v\text{ pol}}$  values are taken from [15] and [20]. —  $p_2$  is derived from equation (15) (respectively Eq. (17)). To calculate the parameter  $m$ , we take  $v_0 = 27.4 + n 26.9 \text{ \AA}^3$ , the volume occupied by one paraffinic chain of  $n$  carbon atoms, and we estimate the surface  $s_0$  occupied by one polar head from [14] [15] and [21]. —  $r_s$  is the value used in the I.P.M.S. fit.

	Lec	Gal	C <sub>16</sub> TAB	KC <sub>12</sub>
$p_1$	0.12	0.10	0.05	0.07
$p_2$	0.13	0.10	0.05-0.1	0.04-0.1
$r_s$	0.098	0.085	0.09	0.09

### Acknowledgments.

We thank C. Oguey and J. F. Sadoc for many fruitful discussions. We are also indebted to A. M. Levelut and B. Pansu for comments.

### References

- [1] International workshop on Geometry and interfaces, E. Dubois-Violette and B. Pansu Eds., Colloque C7, Suppl. n 23, *J. Phys. France* **51** (1990).
- [2] Fontell K., *Colloid Polym. Sci.* **268** (1990) 264.
- [3] Seddon J. M., Hogan J. L., Warrender N. A., Pebay-Peyroula E., *Prog Colloid Polym. Sci.* **81** (1990) 189-197.
- [4] Israelachvili J., Mitchell N. J., Ninham B. W., *J. Chem. Soc. Faraday Trans. II* **72** (1976) 1523-1568.
- [5] Charvolin J., Sadoc J. F., Dubois-Violette E., Pansu B., Geometry in Condensed Matter Physics, J. F. Sadoc, Ed. Vol. **9** (World Scientific. Directions in Condensed Matter, Physics, 1990).
- [6] Charvolin J., Sadoc J. F., *J. Phys. France* **48** (1987) 1559-1569.
- [7] Scriven L. E., *Nature* **263** (1976) 123-125.
- [8] Longley W., Mac Intosh T. J., *Nature* **303** (1983) 612.
- [9] Hyde S. T., Andersson S., Ericsson B., Larsson K., *Zeit. Krist.* **168** (1984) 213.
- [10] Dubois-Violette E., Pansu B., *Mol. Cryst. Liq. Cryst.* **165** (1988) 151 and *Europhys. Lett.* **10** (1989) 43.
- [11] Schoen A. H., Technical Note (1970) NASA TN D-5541 and Not. Amer. Math. Soc. **16** (1969) 519.
- [12] Schwarz H. A., *Gesammelte Mathematische Abhandlungen* (Berlin Springer, 1890).
- [13] Anderson D. M., Davis H. T., Nitsche J. C., Scriven L. E., *Adv. Chem. Phys.* **77** (1990) 337.
- [14] Luzzati V., Spegt P. A., *Nature* **215** (1967) 702.
- [15] Luzzati V., Tardieu A., Gulik-Krzywicki T., Rivas E., Reiss-Husson F., *Nature* **220** (1968) 485.
- [16] Lidin S., Hyde S. T., *J. Phys. France* **48** (1987) 1585.
- [17] Oguey C., Sadoc J. F., *J. Phys. I France* **3** (1993) 839-854.
- [18] Coxeter H. S. M., *Introduction to Geometry* (John Wiley, New-York, 1961).
- [19] Let us note that another model introducing spheres of radius  $R_2$  with a constant density in volume instead of a constant superficial density leads to a parabolic profile in the film  $\rho(z) = \rho_{\max} \left( 1 - \left( \frac{z}{R_2} \right)^2 \right)$ . If we impose the same total paraffinic mass as in the profile of equation (7) we get, after some algebra  $R_s \rho_1 = (2/3) R_2 \rho_{\max}$ . If we choose  $\rho_1 = \rho_{\max}$  this implies  $R_2 = (3/2) R_s$ . The fit of the intensities performed on this model leads to intensities similar to those obtained with the spheres with constant surfacial density. The  $p$  values deduced from the fits are then of the order of 1.5 those obtained in the case of spheres with constant superficial density (see Sect. 4.3), which is in agreement with  $R_2 = 1.5 R_s$ . The  $\alpha$  values are mostly zero, contrary to values obtained in tables II, III and IV. This indicates that contrary to the constant density profile (stiffness), the parabolic one (which is broader) takes into account ab initio fluctuations of the interface.
- [20] Luzzati V., Mariani P., Delacroix H., *Makromol. Chem. Macromol. Symp.* **15** (1988) 1-17.
- [21] Luzzati V., Gulik-Krzywicki T., Tardieu A., *Nature* **218** (1968) 1031.
- [22] Dubois-Violette E., Clerc M., to be published.